A Real-Time Coded OFDM Acoustic Modem in Very Shallow Underwater Communications

Zhong Kun, Quek Swee Sen, Koh Tiong Aik, Tan Bien Aik
DSO National Laboratories, 20 Science Park Drive, Singapore 118230
Email: zkun@dso.org.sg

***Abstract* – In this paper, we describe the design and implementation of a high-rate modem for use in very-shallow water communications. The modem employs an Orthogonal-Frequency-Division-Multiplexing (OFDM) scheme with a powerful forward error-correcting code (FEC) - turbo block code. Bit error rate (BER) measurements obtained from coastal sea trials showed that this modem is capable of delivering good error rate performance for information rates of up to nearly 10 kbits/s at transmission distances below 1700m.**

***Index terms* – Very shallow waters, OFDM, FEC, turbo block code, BER.**

I. INTRODUCTION

In a very-shallow water environment (where the depth of the water is less than 20m and the range-depth ratio is larger than 10:1), commercial modems are able to achieve reliable transmission (i.e., BER<10^{-5}) only at very low data rates (200~300 bps). This poor performance is primarily due to the severe multipaths encountered in very shallow underwater channels. In this paper, we explore the possibility of achieving reliable high rate data communications (1~10 kbps) in very-shallow waters by using the technology of orthogonal frequency-division multiplexing (OFDM) in conjunction with a powerful forward error-correcting code (FEC) – turbo product (block) code (TPC).

OFDM was selected as the modulation scheme because 1) it is simple to cyclically extend each OFDM symbol to eliminate any inter-symbol interference (ISI) due to severe multipaths normally present in very-shallow water channels, 2) OFDM is robust against impulsive shrimp noise, and 3) actual channel measurements from stationary positions revealed that the Doppler spread in the channel is mild enough for OFDM not to suffer any significant performance loss due to inter-carrier interference (ICI) [1-3]. As the Doppler spread is small, the channel can be considered static across two consecutive OFDM symbols and differential PSK (DPSK) modulation could be used on each sub-carrier. The advantage of employing the DPSK modulation is that it does not require any channel estimation at the receiver and therefore greatly reduces the implementation complexity.

However, OFDM technology alone cannot ensure reliable transmission due to frequency selectivity on the OFDM sub-carriers introduced by the channel multipaths. This results in the DPSK signals on some of the sub-carriers being so severely attenuated that reliable detection is simply not possible. As such, FEC has to be applied to introduce redundancies across the sub-carriers in the hope that those information bits undergoing deep-fades in the frequency domain can be recovered through the channel decoding process.

Turbo codes and the associated iterative decoding techniques have generated much interest within the research fraternity in recent years for their ability to achieve an exceptionally low BER with a signal to noise ratio per information bit close to Shannon's theoretical limit on a Gaussian channel [4]. TPC was selected as the FEC due to its powerful error-correction capability based on soft-input-soft-output (SISO) iterative decoding algorithm and its excellent BER performance at high code rate (> 0.65) [5]. Implementation-wise, TPCs are less complex than Berrou's turbo convolutional codes, with the Chase Algorithm simplifying the decoding effort required for TPCs [6].

This paper is organized as follows. In section II, the coded OFDM modem architecture is described. In section III, sea trial setup and channel measurements are presented. Section IV then describes the performance of the automatic gain control (AGC), time synchronization performance and the BER performance. Section V presents the conclusions of the paper.

II. MODEM ARCHITECTURE

A. Overview.

As shown in Fig.1, the modem comprises of three major modules: 1) the Graphical User Interface (GUI), TPC encoder and decoder, and an optional interleaver/deinterleaver for TPC all implemented in C++ on a personal computer (PC); 2) the OFDM transmitter and receiver implemented in VHDL on a Field Programmable Gate Array (FPGA) circuit board; and 3) the electrical/acoustic converter chains. During transmission, the user data is first encoded by the FEC encoder and then passed to the OFDM transmitter via the PC/FPGA data interface. The OFDM transmitter output samples are then fed into the DAC to yield the analog waveform which is subsequently amplified, filtered and converted to an acoustic signal by the projector. During reception, the acoustic signal is converted to electrical signal by the receiver hydrophone before entering the signal conditioning board and ADC. The ADC output samples are processed by the OFDM receiver which passes soft reliability information of the received bits to the FEC decoder via the FPGA/PC data interface. The FEC decoder then produces at its output the estimate of the user data.

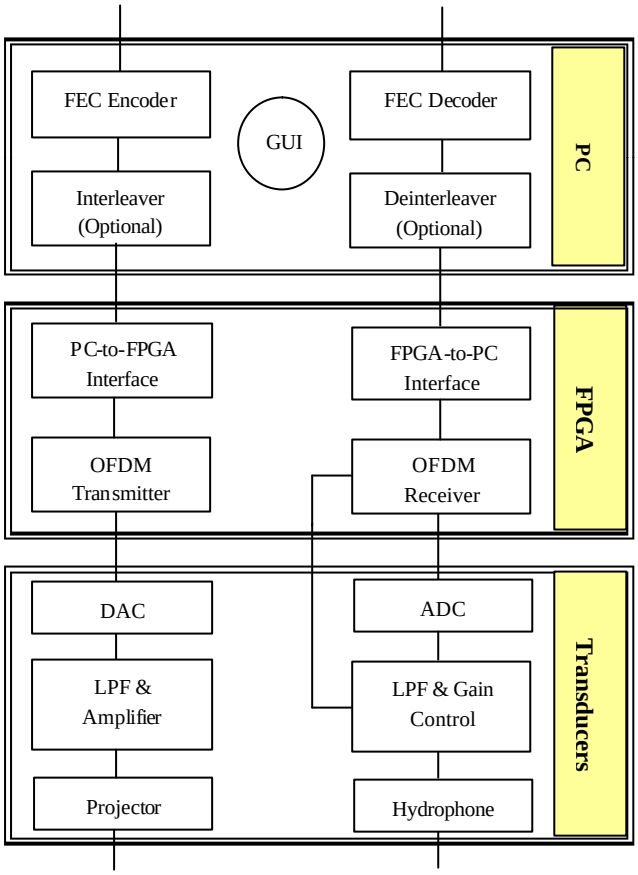

Fig.1 Overview of the modem architecture.

B. Waveform Structure.

The OFDM waveform is organized into bursts. Each burst is preceded by an AGC preamble that is followed by OFDM data frames. Each frame starts with a time synchronization preamble. The synchronization preamble is then followed by OFDM training symbols that are used by the receiver for frequency offset estimation and compensation [7]. The training symbols are designed such that the training portion of the OFDM waveform has a low peak-to-average power ratio [8] in order for the frequency offset estimation to be less affected by any possible nonlinearity present in the transducers. The training symbols are followed by OFDM data symbols. The frame structure of the OFDM waveform is depicted in Fig.2. Cyclic extensions are included within each OFDM data symbol to prevent inter-symbol interference (the cyclic extensions of the OFDM symbols are not shown in the Fig 2).

C. OFDM Transmitter.

The transmitter consists of a time-domain Gray-coded differential QPSK (DQPSK) modulator that takes two FEC encoded data bits at a time and produces a complex-valued sample corresponding to one of the four QPSK constellation points.

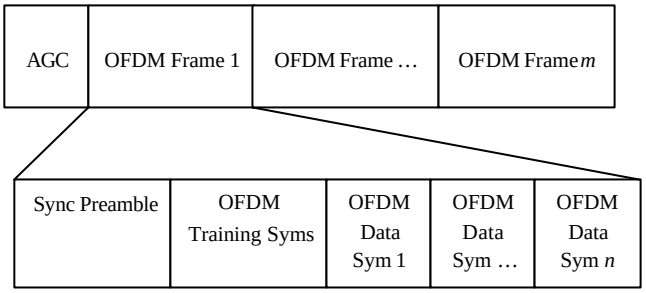

Fig.2 OFDM frame structure.

The modulator output samples together with guard channels (to cater to non-ideal filters) are subsequently applied to a 64-point IFFT. The IFFT output samples are then cyclically extended and mixed with the signal samples from the AGC and synchronization preamble generators according to the frame structure described in Fig.2. The framed baseband signal is fed to a digital up converter (DUC) [9] that performs signal interpolation, lowpass filtering and frequency translation. The DUC output is then connected to the DAC. The major design parameters of the OFDM transmitter are summarized in Table.1 below.

Table.1 Design parameters of the OFDM transmitter.

Total number of sub-carriers	64
Total number of OFDM symbols per frame	20
Sub-carrier modulation scheme	DQPSK/DBPSK
Duration of one OFDM frame (including time sync preamble)	137.2 or 320.4ms
FEC code rate	0.75
Transmission data rate averaged over one burst, R_T	12.722kbps (1) 6..361kbps (2) 5.544kbps (3) 2.772kbps (4)
Information data rate averaged over one burst, R_{user}	$0.75 \times R_T$

*(1) For DQPSK, short cyclic extension; (2) for DBPSK, short cyclic extension; (3) for DQPSK, long cyclic extension; and (4) for DBPSK, long cyclic extension.

D. OFDM Receiver.

The first stage of the OFDM receiver is the AGC unit. The AGC is used to ensure that the signal has a voltage level that is compatible with and makes the best use of the dynamic input range of the ADC. Discussions on the AGC performance are presented in Section III. The AGC unit is followed by a digital down converter (DDC) that performs signal frequency translation to baseband, lowpass filtering and sampling rate decimation [9]. The DDC baseband output is then fed into both the frame synchronization unit and the frequency offset compensation (FOC) unit simultaneously. The frame synchronization unit correlates the incoming signal with the

known time-sync sequence. Upon successful frame synchronization, the FOC unit starts to estimate and compensate for the frequency offset using the OFDM training symbols. The cyclic extensions of the frequency-offset-corrected signal samples are then removed and the useful portions of the OFDM data symbols are fed into the FFT processor. The DPSK demodulator mu ltiplies the FFT output samples on the data sub-carriers with the conjugates of the samples on the corresponding data sub-carriers in the previous FFT output block in the same frame. The DPSK demodulator then passes the reliability information of the demodulated bits to the channel decoder.

E. FEC.

The TPC encoder structure is illustrated in Fig.3. For TPC encoding, a total of 676 information bits are placed into a $k \times k$ array. Then a single-parity-check code is applied to every row of the array to result in a $k \times n$ matrix and subsequently the same code is applied to every column of the resultant matrix to yield an $n \times n$ matrix that contains 900 bits (a so-called product code). The code rate is $k^2/n^2 \sim 0.75$. For DQPSK modulation, each OFDM frame contains two TPC code blocks; and for DBPSK modulation, each OFDM frame contains just one TPC code block.

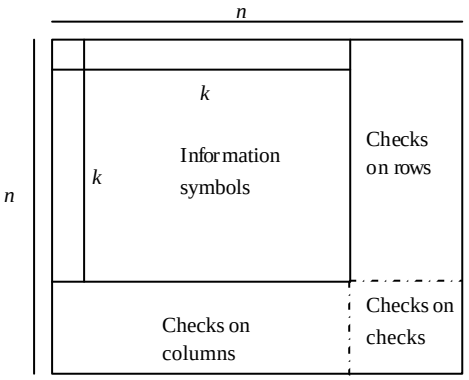

Fig.3 Turbo product code (TPC) encoder structure.

The TPC decoding is based on soft-input soft-output iterative algorithms and the details can be found in [5].

III. SEA TRIAL SETUP & CHANNEL DELAY PROFILES

A. Trial Setup.

The sea trial was conducted in the coastal sea off Singapore in 2005. In the sea trial, the receiving ship, ship B, remained at a fixed position while the transmitting ship, Ship A, moved to different locations that are at distances of 400m, 1000m, 1700m and 2500m away from the receiving ship. The sea trial setup is graphically illustrated in Fig.4.

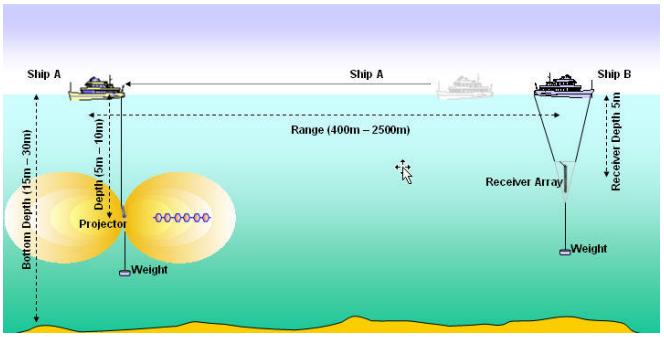

Fig.4 Sea trial setup.

B. Channel Power Delay Profiles.

Earlier channel measurements showed that the channel displays much stronger multipath spread at near ranges (<1000m) than at far ranges (>1500m). This is verified by the multipath power delay profiles (20dB margined) obtained by transmitting single-carrier pseudo-random sequence and correlating the received sequence with the reference sequence. Two multipath power delay profiles at distances of 400m and 1700m are plotted in Fig.5. It can be observed that severe multipaths are present at short distances.

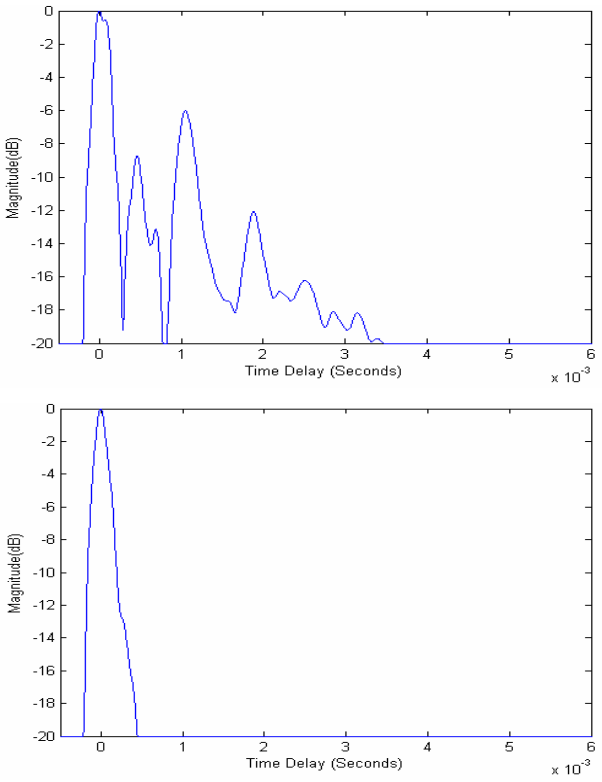

Fig.5 Channel power delay profiles at distances 400m (upper plot) and 1700m (lower plot).

IV. AGC, TIME SYNC & BER PERFORMANCE

A. AGC Performance.

Fig.6 is a snapshot of the AGC output during the sea trial. It shows the instantaneous gain computed by the AGC module as a function of time. Three distinct modes of the AGC can be seen from the figure. During the *acquisition* mode, the AGC gain is randomly fluctuating when only noise is present at the receiver front end. Once the AGC preamble is received, the AGC gain will be quickly adjusted to converge to a constant value that can enable a good use of the dynamic range of the ADC. The AGC will converge to the constant mode and remain in this mode during the reception of OFDM portions of the received signal. The AGC will enter the tracking mode to allow the gain to be adapted to small changes in received signal strength during the reception of the time synchronization preambles between OFDM frames in one burst.

B. Time Synchronization Performance.

Fig.7 includes two snapshots during the sea trial at distances of 400m and 1700m, respectively. It shows time timing synchronization output power as a function of time. Note the close resemblance between the plots in Fig.7 and the corresponding plots in Fig.5 where the channel power delay profiles were shown. However, there are some small peaks in the plots of Fig.7 that are absent in the corresponding plots of Fig.5, these small peaks can be attributed to the non-zero cross correlation between the OFDM portion of the received signal and the known synchronization preamble.

C. BER Measurements

The BER measurement results at the three distances of 400m, 1000m and 1700m are tabulated in Table.2. For 1700m, the short cyclic extensions are used in the transmitted OFDM waveform; while for the other two distances, the long cyclic extensions are used.

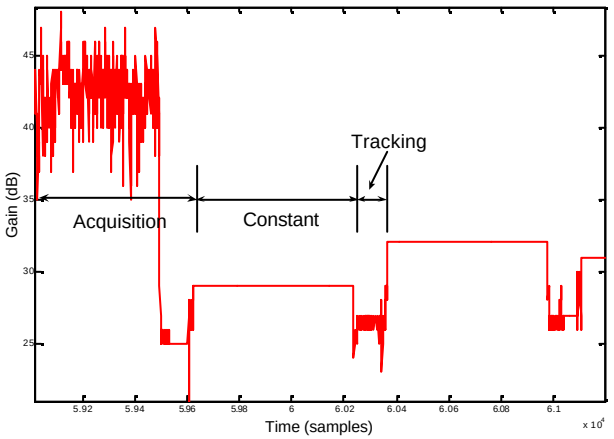

Fig.6 Snapshot of the AGC performance in real-time transceiving.

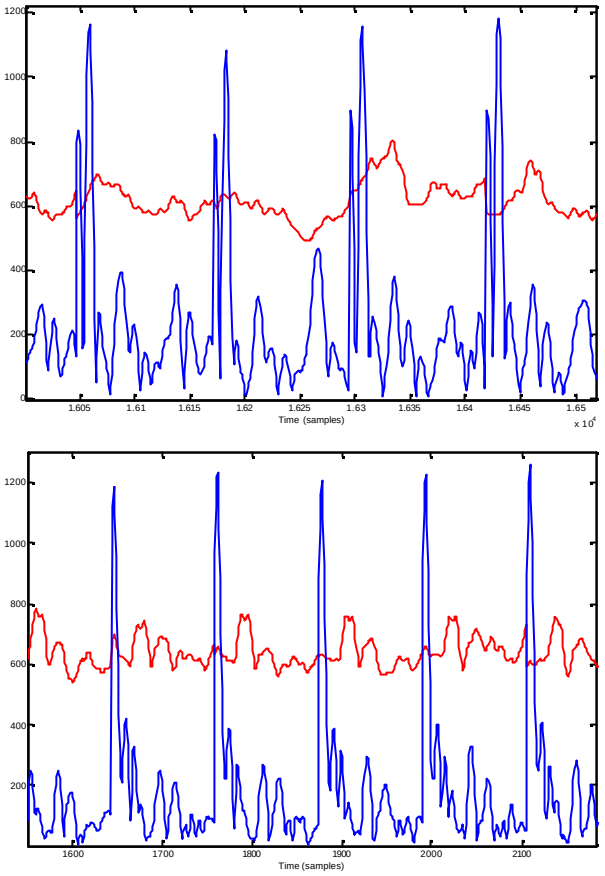

Fig.7 Time synchronization correlator output power vs. time at distances of 400m (upper) and 1700m (lower).

From Table.2 it can be seen that at far range, the modem can deliver much higher user data rate than at near range. Also, through offline analysis it was found that at shorter ranges, as the delay spread becomes more severe there are more spectral nulls on the data sub-carriers which prevents the use of DQPSK (DQPSK only delivered an average coded BER in the order of 1e-3 to 1e-2 for 400m). On the other hand, when the distance was increased to 2500m, the coded OFDM failed to achieve reliable transmission (BER ~ 1e-2). This could be explained as follows. Since the OFDM waveform has a relatively large peak-to-average power ratio, the average transmit power has to be kept low in order to ensure the transmitted OFDM waveform is not clipped at the transducers (from DAC to projector) to cause any nonlinear distortion. Thus, at long distances (e.g., 2500m), there is simply insufficient signal-to-noise ratio (SNR) to ensure reliable transmission even though the channel maximum delay spread is just a fraction of the length of the short cyclic extension. This is verified by the power spectral density (PSD) plot of the received OFDM baseband signal at 2500m as shown in Fig.8.

Table.2 BER measurements for distances of 400m, 1000m and 1700m.

Range (m)	R_{user} (kbps)	Mod	BER
400	2.082	DBPSK	<5e-5
1000	2.082	DBPSK	<4e-6
1000	4.164	DQPSK	<4e-6
1700	4.778	DBPSK	<4e-6
1700	9.555	DQPSK	<4e-6

V. CONCLUSIONS

This paper described the waveform structure and architecture of a COFDM acoustic modem. Our initial measurements revealed that this modem has the potential of delivering high data rates at distances below 1700m in a very shallow water environment. However, the data rate drops as distance decreases because longer cyclic extensions are needed to avoid ISI caused by larger channel delay spreads at shorter distances and lower-order signal constellation has to be used on the sub-carriers as the number of spectral nulls increases. At longer distances, this modem ceases to provide reliable transmission due primarily to insufficient SNR. This is compounded by the fact that the OFDM waveform's large peak-to-average power ratio (as compared to single-carrier modulations) requires a significant input power backoff for the modem to operate in the linear region of the amplifier. Development is currently on-going to resolve these implementation issues.

ACKNOWLEDGMENT

We would like to thank Dr. Ng Boon Chong and Mr. Chia Chin Swee for their invaluable advice during the entire course of this work.

REFERENCES

[1] A. R. S. Bahai, B.R. Saltzberg, and Mustafa Ergen, *Multi-Carrier Digital Communications – Theory and Applications of OFDM*, 2nd ed., Springer, 2004.

[2] Nee, R. and Prasad, R., *OFDM for Wireless Multimedia Communications*, Artech House, January 2000.

[3] Bingham, J. A. C., *ADSL, VDSL, and Multicarrier Modulation*, New York: Wiley, 2000.

[4] Berrou, C. and Glavieux A., "Near optimum error correcting coding and decoding: turbo codes", *IEEE Transactions on Communications*, Vol.44, Issue 10, pp. 1261-1271, Oct 1996.

[5] Pyndiah, "Near-optimum decoding of product codes: block turbo codes", *IEEE Transactions on Communications*, Vol.46, Issue 8, pp.1003-1010, Aug 1998.

[6] Chase, D., "Class of algorithms for decoding block codes with channel measurement information", *IEEE Transactions on Information Theory*, Vol.18, Issue 1, pp.170-182, Jan 1972.

[7] Haiyun Tang, Lau, K. Y., and Brodersen, R. W., "Synchronization schemes for packet OFDM," *ICC'03*, Vol.5, pp.3346-3350, May 2003.

[8] Tarokh, V. and Jafarkhani, H., "An algorithm for reducing the peak to average power ratio in a multicarrier communication system", *IEEE 49th VTC*, pp.680-684, May 1999..

[9] E. B. Hogenauer, "An economical class of digital filters for decimation and interpolation," *IEEE Trans. on Acoustics, Speech, and Signal Processing*, Vol.ASSP-29, No.2, pp.155-162, April, 1981.

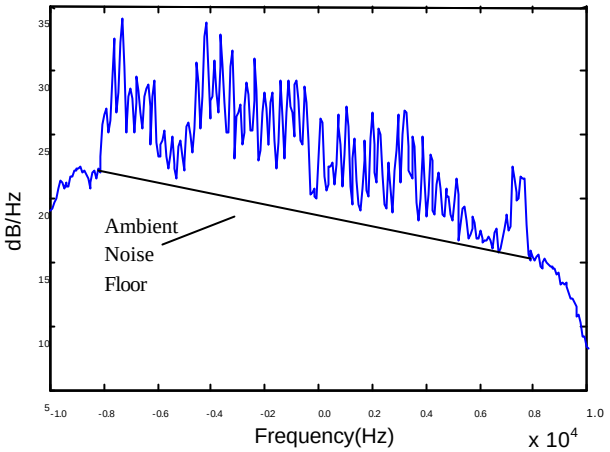

Fig.8 PSD plot of the received baseband OFDM signal at distance 2500m.